PROCEEDINGS OF SCIENCE

Dark matter searches with the full data sample of the ANTARES neutrino telescope

Sara Rebecca Gozzini[a,*] **and Juan de Dios Zornoza**[a] **on behalf of the ANTARES Collaboration**

[a] *IFIC - Instituto de Física Corpuscular (CSIC - Universitat de València), c/Catedrático José Beltrán, 2, 46980 Paterna, Valencia, Spain*

E-mail: sara.gozzini@ific.uv.es, zornoza@ific.uv.es

Extraterrestrial neutrinos can be used to probe the presence of dark matter in the Milky Way. Pair annihilation and decay of dark matter particles could give rise to sizable fluxes of high-energy neutrinos detectable with large volume Cherenkov telescopes. The Galactic Centre is one of the most promising sources for these searches. Telescopes installed in the Mediterranean Sea are best suited to look for dark matter from this source. Another interesting source to study is the Sun, given its proximity. Moreover, it is a source almost free of astrophysical background. The ANTARES neutrino telescope has been taking data in the Mediterranean, offshore the French coast, for 16 years and has been decommissioned in 2022. The detector had a very good resolution in determining the direction and energy of the incoming neutrinos. The expected space and energy distributions of dark matter overdensity regions are used to characterise the searched signal over a (known) diffuse background of atmospheric neutrinos. In this contribution we present the most relevant results of dark matter searches with the full ANTARES data sample. A search for signatures of Weakly Interacting Massive Particles (WIMPs) has been performed with electron- and muon-neutrino data, in an energy range from 50 GeV/c^2 to 100 TeV/c^2. All these searches set competitive upper limits on the strength of dark matter pair annihilation which are reported here.

38th International Cosmic Ray Conference (ICRC2023)
26 July - 3 August, 2023
Nagoya, Japan

*Speaker

PoS(ICRC2023)1375

1. Introduction

Dark matter makes up to 27% of the Universe mass-energy budget, and it is plausible to describe this additional matter contribution in terms of a new fundamental particle, fitting it in an extension of the Standard Model [1]. However, all microscopic searches for a neutral particle, stable on cosmological scales, and whose relic abundance fits astronomical observations have until now come up empty-handed. Left apart these basic properties, the particle mass and interaction strengths are unconstrained over a wide range of values. The main candidates for neutrino-based searches are weakly interacting massive particles (WIMPs), that naturally display an interaction strength of the same order as the known electroweak interaction, and could therefore be a target for neutrino telescopes. For this kind of *indirect* searches, neutrino flux predictions from pair annihilations or decays of WIMPs are provided by tools such as PPPC4DMID [2] or WIMPSim [3]; these lookup tables supply the energy distributions of neutrino final states in a straight-forward format for being included in the instrument's Monte Carlo simulations, as detailed in section 3. As for the source morphology, the Earth moves in the Galactic dark matter halo; searches performed with neutrinos target directly the main accumulation point at the Centre of the Milky Way, or, alternatively, massive nearby celestial bodies (such as the Sun) where WIMPs from the same Galactic halo are supposed to be trapped interacting with nucleons in the star's interior, up to a condition of equilibrium between their capture and annihilation rates. The amount of dark matter inside an extended source such as the Galactic Centre is characterised with the J-factor $J = \int_\Omega d\Omega \int_l \rho^2(r(\theta,\phi))dl$, expressing the dark matter density integrated over a viewing angle Ω and along the line of sight l, at the celestial coordinates θ and ϕ. The shape of the dark matter halo for extended sources is described with models built around astrophysical data, or taking input from N-body simulations, such as Navarro-Frenk-White (NFW) [4]. This is used as a benchmark for the Galactic Centre analyses presented here, numerically evaluated with CLUMPY [5]. As for the mass of the dark matter candidate, in the searches presented here there is no prior assumption on this parameter that is considered to span values up to 100 TeV/c^2. A lower bound on the WIMP mass tested is instead due to the energy threshold proper of the geometry and spacing of the detector; this threshold is about 25 GeV for ANTARES, as detailed in section 2. One final *caveat*: indirect searches are largely affected by systematic uncertainties mostly coming from the parametrisation of the dark matter halo profile, which makes the triangulation between search methods (direct, indirect, production) compelling in case of a signal appearance. Taking account of this, neutrino telescopes, which are not originally designed for dark matter searches, are able to place competitive limits.

2. Instrument

ANTARES was a very-large volume Cherenkov neutrino detector, in fact the first underwater instrument of this type, built as an array of photomultiplier tubes installed in the Mediterranean Sea, 40 km offshore from the French coast at Toulon. This detector instrumented about 0.1 km^3 of water, with a layout of 12 detection lines each with a length of 450 metres, anchored to the seabed at a depth of 2500 metres. A total of 885 optical modules, meaning photomultiplier tubes crated in pressure-resistant glass spheres, were arranged on the lines at a spacing of 14.5 metres from one another, leaving about 60 metres between neighbouring lines. ANTARES was cabled to shore and

served by the shore station and control room at La Seyne-sur-mer (France); for a detailed technical description see [6]. The spacing between optical modules determines a minimum energy threshold for an event to trigger a signal. The ANTARES telescope was conceived for neutrino astronomy: its layout was optimised to detect energies between a few tens of GeV and 10^6 GeV. This energy window is exploited for dark-matter searches in its lower to middle range. From its geographical position at 42°48'N, 6°10'E, this instrument has a coverage of Galactic Centre, where the dark matter density is predicted to be the highest, for about 70% of the time. ANTARES was switched off in February 2022 and entirely removed from the sea. The entire data set, from *first light* in 2007 to decommissioning in 2022, was used to search for dark matter signatures.

3. Data Structure and Selection

In ANTARES one data event appears as a pattern of light signals caused by the Cherenkov photons radiated by a relativistic leptons propagating inside the instrumented volume of the detector. If the lepton is upward-going, it must have been produced in a weak process such as the interaction of a neutrino on a nucleon in the vicinity of the instrumented volume. The position and the time of each light signal are recorded. The signatures left by electrons and muons in ANTARES were spherically-shaped (*showers*) and linearly-shaped (*tracks*), respectively. Through reconstruction of arrival direction, shape, and amount of deposited light of the daughter lepton track, it is possible to backtrack the neutrino observables (incoming direction, flavour and energy, respectively). The data set analysed for this dark matter search covers an effective livetime of 4532.16 days, and was composed of both tracks and showers. Indeed, dark matter pair-annihilations yield the three flavour ν_e, ν_μ and ν_τ as final states. Despite ANTARES being by design optimised for the detection of track-like events induced by charged current interactions of ν_μ, a small percentage of showers is present in the data. As a note, the pre-selection of showers was not optimised for WIMP annihilation signatures here, but reproduces the selection adopted for astrophysical neutrino searches.

Dark matter searches rely on Monte Carlo simulations to profile the signal as it would appear in ANTARES. Sets of simulated data have been produced in correspondence with the environmental and trigger conditions of each *run* (about 12 hours) of data acquisition. The features of dark matter signals are obtained with appropriate *weights* that modulate the energy and spatial distribution of events, according to each combination of input parameters (annihilation mode, halo profile). An additional caveat: WIMP dark matter is tested here in its most universal and comprehensive scenario, which does not consider the model-dependent cross section for each of the final states exclusively, meaning that each of the annihilation channels searched here is considered independently of the others with a 100% branching ratio. The investigation of model-specific features of the annihilation modes goes beyond the reach of this search.

Data are preselected upon quality criteria using indicators of the track or shower reconstruction quality as summarized in Table 1. Here the subscripts AA, T stands for the reconstruction algorithm used for tracks and shower variables respectively. The benchmark reference sample obtained with indicators of the track or shower reconstruction quality in Table 1 contains 11850 tracks and 235 showers. Cuts in Table 1 are applied to all combinations of WIMP input parameters; additionally, a cut on the number of hits (N_{HIT}) in each event is optimised for each of the WIMP parameter combination. Indeed, the energy distribution of two annihilating WIMPs (or any 2

High track likelihood	$\Lambda_{\mathrm{AA}} > -5.2$
Small angular error	$\beta_{\mathrm{AA}} < 1^\circ$
Upgoing	$\cos(\theta_{\mathrm{AA}}) > -0.1$
High shower likelihood	$\mathrm{lik}_T > 50$
Time residual fit matches shower geometry	$M_T < 1000$
Small enough angular error	$\beta_T < 10^\circ$
Upgoing	$\cos(\theta_T) > 0.0$
Vertex confinement	$\sqrt{x_T^2 + y_T^2} < 300\mathrm{m}, \lvert z_T \rvert < 250\mathrm{m}$

Table 1: Selection criteria adopted for track candidates (top block) and shower candidates (bottom block). For tracks, the variable used are the likelihood of a line fit Λ_{AA}, the angular error estimate β_{AA}, and the reconstructed anti-zenithal angle of the event θ_{AA}. For showers, the variables used are the likelihood of a spherical fit lik_T, the time residual with respect to a spherical geometry M_T, the angular error estimate β_T, the reconstructed anti-zenithal angle of the event θ_T, and the coordinates of the event vertex x_T, y_T and z_T required to be contained inside a cylinder contained inside the detector volume.

particles $\rightarrow$ 2 particles spectrum, more generally) displays distinctive features that would provide the overwhelming evidence for this kind of signal, when compared with the atmospheric neutrino background whose spectrum follows a decaying power law. While ANTARES has a dedicated energy estimator, this estimator performs best for mid- to high-energy events, with long tracks. For our analysis, we therefore use the number of hits N_{HIT} which provides a calorimetric, yet not absolutely calibrated, proxy for the event's energy. An additional energy dependent selection best exploits the shape of the WIMP annihilation spectra. Note that this energy selection is characteristic of dark matter searches and cannot be profitably applied, for instance, to searches for astrophysical neutrino signals. The cut on N_{HIT} is varied, choosing between values corresponding to a reduction of the total signal acceptance to 90%, 75%, 50% and 25%; for WIMP each parameter combination, the value leading to the best sensitivity are used.

3.1 Signal: WIMP Pair Annihilation at Neutrino Telescopes

The expected dark matter annihilation signal at ANTARES is obtained reweighting Monte Carlo simulated events to match the energy distribution of WIMP pair annihilation, and distributing them around the position of the Galactic Centre according to the shape of a given dark matter halo profile, folding in the detector resolution.This analysis uses the energy distributions from the PPPC4DMID tables [2] for the single WIMP collision, and the NFW halo profile [4]. Five channels are considered with independent 100% branching ratio each: WIMP WIMP $\rightarrow \tau^+\tau^- \rightarrow \nu\bar{\nu}; \mu^+\mu^- \rightarrow \nu\bar{\nu}; b\bar{b} \rightarrow \nu\bar{\nu}; W^+W^- \rightarrow \nu\bar{\nu}; \nu\bar{\nu}$. The complete process takes place inside the source, which the final products leave already as neutrinos, allowing to neglect energy distortion due to absorption. The neutrino yield obtained with PPPC4DMID is then oscillated in the long baseline approximation between the source and the detection site.

3.1.1 Acceptance, flux, cross-section

The effective area associated with an analysis represents the equivalent surface of the detector once accounted for cross section and detection probability of the secondary leptons, detector geometry, trigger efficiency and the analysis cuts. As both the effective area and the WIMP annihilation spectra are energy dependent, folding those two distributions gives a measurement of

the differential acceptance, or the probability for the detector to record an event of a given energy. The integrated acceptance is obtained as the effective area modulated through each annihilation spectrum, dN_ν/dE_ν, integrated between the energy threshold of the detector and the WIMP mass M:

$$\mathcal{A}(M) = \int_0^M A^\nu_{eff}(E_\nu)\frac{dN_\nu(E_\nu)}{dE_\nu}dE_\nu + A^{\bar{\nu}}_{eff}(E_{\bar{\nu}})\frac{dN_{\bar{\nu}}(E_{\bar{\nu}})}{dE_{\bar{\nu}}}dE_{\bar{\nu}}. \tag{1}$$

The knowledge of the detector effective area will allow us to constrain or measure the neutrino flux from dark matter annihilation, as described in section 4.

3.2 Background

Once removed the events with poor reconstruction quality, the spurious coincidences (electronic noise, bioluminescence) and the atmospheric muons, the remaining background consists of atmospheric neutrinos. This is an irreducible background distributed isotropically in right ascension, which follows a decreasing power-law energy spectrum. In this analysis, the background is not simulated with Monte Carlo but directly obtained from data after a random shuffling of the right ascension coordinate. This shuffling ensures that any possible signal clusters present in the data is washed out.

4. Statistical analysis

This indirect dark matter search is structured as a hypothesis test, with a signal hypothesis H_1, where a cluster of n_s neutrino events originate from pair annihilation of WIMPs, is tested against a null hypothesis H_0, where all N_{data} neutrinos in the data sample are produced in the Earth's atmosphere. The number of expected signal events n_s is *a priori* unknown and is varied between 1 and 50, identifying the best-fit value n_s^* with an unbinned maximum likelihood method. Pseudo-experiments are realised injecting n_s signal events on top of $n_b = N_{data} - n_s$ background events, drawn from blind data to reproduce the background. N_{data} represents the number of events surviving the cuts in the data sample, for each parameter combination. A likelihood function characterising each data set (pseudo-data set for determining the sensitivity, and real data set after unblinding) is defined as

$$\mathcal{L}(n_s) = \prod_i^{n_{datad}} \left[n_s \cdot P_s(\text{angle}, N_{\text{HIT}}, \beta) + n_b \cdot P_b(\text{angle}, N_{\text{HIT}}, \beta)\right], \tag{2}$$

where P_s and P_b are probability density fuctions (PDFs) for signal and background respectively. The index i runs over all the events in the pseudo-set. As both track and shower candidates are included, the number of signal and background events is split into a relative fraction of tracks and showers that reflect the acceptance ratio, for each WIMP mass and annihilation channel considered. Tracks and showers have two distinct sets of PDFs. The discriminant variable to evaluate the significance of a signal cluster is the test statistic TS defined as the ratio between the maximum likelihood and the likelihood of the background hypothesis $\mathcal{L}_{BG} = \mathcal{L}(n_s = 0)$:

$$TS = -\log\left(\frac{\mathcal{L}(n_s^*)}{\mathcal{L}_{BG}}\right). \tag{3}$$

Following Neyman's prescription [7], the analysis sensitivity is obtained as the average upper limit at 90% confidence level, computed comparing the median TS of the background case with each distribution $P(TS)$ for each pseudo-experiment set.

The number of events in each set of pseudo-experiments is subject to fluctuations following a Poisson distribution. To include this effect, a transformation through a Poisson function $\mathcal{P}$ is performed, returning the TS as a function of the Poissonian mean μ as $P(TS(\mu)) = P(TS(n_s^*)) \times \mathcal{P}(n_s, \mu)$. A 15% systematics on the number of detected events is expected with ANTARES [8]. This effect is included folding the above equation with a Gaussian smearing of 15% width. At a first stage, cuts are optimised aiming for best sensitivity, keeping the data set *"blind"* (i.e. with the event coordinates randomly shuffled in right-ascension). After assessment of the best cuts for each combination of WIMP mass and annihilation channel, data is unblinded with those cuts; as 18 mass values were tested for the μ, τ, b, ν channels, and 17 for the W channel, 89 unblindings have been performed.

5. Results of Dark Matter Searches

When testing the dark matter hypothesis in the Galactic Centre, ANTARES data is found to be consistent with background for all WIMP parameters combinations. Upper limits obtained with the complete data set of 4532.16 days livetime are shown in Figure 1 for all the WIMP masses and annihilation channels searched. These results are under the assumption that each annihilation channel is considered exclusively with 100% branching ratio, and are affected by systematic uncertainties in the dark matter halo model.

The Sun is also an accumulation point for dark matter targeted with neutrino telescopes. WIMPs can have two types of interactions with ordinary matter: spin-dependent, coupling to the spin of the target nucleon, and spin-independent, coupling to its mass [10]. The two of them can take place inside the Sun that contains both light elements with an odd number of nucleons, like hydrogen, and relatively heavy elements, like Helium and Oxygen. Through either process, WIMPs are captured inside the Sun where their density raises until equilibrium, when capture rate equals the rate of annihilation into Standard Model particles, making the Sun a source of a continuous neutrino flux from WIMP annihilation. The final states energy spectra undergo further distortions due to the amount of dense matter to cross before leaving the Sun's surface, and are computed using WIMPSim [3]. ANTARES have searched their 2007-2019 data set using tracks coming from the direction of the Sun, and placed upper limits on the presence of dark-matter induced events both for spin-dependent and spint-independent interactions [13].

Acknowledgements

The authors acknowledge the support from grants Ministerio de Ciencia e Innovación (MCIN): Programa Estatal para Impulsar la Investigación Científico-Técnica y su Transferencia - Subprograma Estatal de Generación de Conocimiento (reference PID2021-124591NB-C41), PID2021-124591NB-C43 funded by MCIN/AEI/10.13039/501100011033 and by "ERDF A way of making Europe", European Union; Generalitat Valenciana: Programa Santiago Grisolía (GRISOLIAP/2021/192, 2021-2025), and Program GenT (ref. CIDEGENT/2021/023).

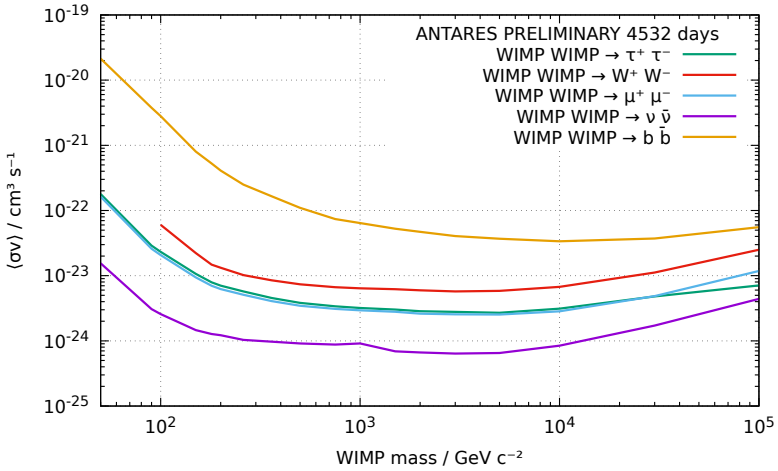

Figure 1: Upper limits at 90% confidence level on the thermally averaged cross section for pair annihilation of WIMPs resulting to neutrinos. For low WIMP masses, previous results [9] also contain a dedicated reconstruction fit (χ^2 based, for events reconstructed on single-line data. This work, that improves the sensitivity for low masses, is in progress for the complete data set.

References

[1] G. Bertone. Particle Dark Matter : Observations, Models and Searches, Cambridge University Press 978-0-521-76368-4 (2010)

[2] M.Cirelli, G.Corcella, A.Hektor, G.Hütsi, M.Kadastik, P.Panci, M.Raidal, F.Sala, A.Strumia, arXiv 1012.4515, *Journal of Cosmology and Astroparticle Physics* **1103** (2011) 051.

[3] Mattias Blennow *et al.* JCAP **01** (2008) 021

[4] J. F. Navarro, C. S. Frenk and S. D. M. White, Astrophys. J. **462** (1996), 563-575

[5] A.Charbonnier, C.Céline, D.Maurin, *Computer Phys. Comm.* **183.3** (2012): 656-668.

[6] M. Ageron *et al.* [ANTARES Collaboration], Nucl. Instrum. Meth. A **656** (2011), 11-38

[7] J. Neyman, *Philosophical Transactions of the Royal Society of London. Series A, Mathematical and Physical Sciences* **236** 1937 333–380.

[8] A. Albert *et al.* [ANTARES Collaboration], Phys. Rev. D **96** (2017) no.8, 082001

[9] A. Albert *et al.* [ANTARES Collaboration], Phys. Lett. B **805** (2020)

[10] A. H. G. Peter, Phys. Rev. D, **79** (2009), 10, 103531

[11] A. Albert *et al.* [ANTARES Collaboration], JCAP **06** (2022) 018

[12] T. Bringmann, J. Edsjö, P. Gondolo, P. Ullio and L. Bergström, JCAP **1807** (2018) 033

[13] A. Albert *et al.* [ANTARES Collaboration], in preparation.